The Role of Protein–Plasticizer–Clay Interactions on Processing and Properties of Thermoplastic Zein Bionanocomposites

I. Nedi,[1] E. Di Maio,[1] S. Iannace[2]

[1]*Department of Materials and Production Engineering, University of Naples Federico II, P.le Tecchio 80, 80125 Naples, Italy*
[2]*Institute for Composite and Biomedical Materials (IMCB)-CNR, P.le Tecchio 80, 80125 Naples, Italy*

Received 14 October 2011; accepted 21 January 2012
DOI 10.1002/app.36860
Published online in Wiley Online Library (wileyonlinelibrary.com).

ABSTRACT: Bionanocomposites (BNCs) based on thermoplastic zein (TPZ) and unmodified sodium montmorillonite (MMT), at 1, 2.5, 5, and 10 wt % loading, were prepared by using an internal mixer. The nanocomposites were characterized by using the following analytical methods: small-angle and wide-angle X-ray diffraction, thermogravimetric, dynamic-mechanical and mechanical analyses. Results evidenced that the efficient dispersion of the inorganic reinforcement, as proved by X-ray diffraction, allowed for an effective improvement of thermal and mechanical properties of the BNCs with respect to the neat TPZ. In particular, a significant increase of the storage modulus in the whole temperature range was observed in dynamic-mechanical experiments. A dramatic increase of mechanical properties has also been observed, with Young's modulus increasing from 296 MPa for neat TPZ to 1205 MPa at 5 wt % and to 1478 at 10 wt % of MMT. The observed dependencies are explained by means of three concurring mechanisms: (i) the stiffening by exfoliated MMT platelets, (ii) the development of strong interactions between the nanoparticles and the protein macromolecules, promoted by the low-molecular weight plasticizer, (iii) the occurrence of possible plasticizer sequestration by MMT and the corresponding reduction of plasticizing effect on the protein. © 2012 Wiley Periodicals, Inc. J Appl Polym Sci 000: 000–000, 2012

Key words: nanocomposites; mechanical properties; thermogravimetric analysis (TGA); X-ray diffraction (XRD); protein, TEM

INTRODUCTION

Use of polymers from renewable resources for packaging applications is steadily growing. Polymers directly extracted/removed from biomass such as polysaccharides and proteins, besides the natural origin, have the additional advantage of being biodegradable and/or compostable under specific environmental conditions. However, when compared to thermoplastic synthetic polymers, they present problems associated to processing and to reduced performances in terms of functional and structural properties. In particular, processing problems are relevant for biopolymers directly extracted from biomass (e.g., cellulose, polysaccharides, and proteins), mainly due to limited plastic-flow properties of these polymers and the intrinsically difficult reproducibility and control over the molecular architecture and spatial conformation of the natural macromolecule.

Correspondence to: E. Di Maio (edimaio@unina.it).

Contract grant sponsor: Commission of the European Communities, Framework 6, Priority 5 "Food Quality and Safety" Integrated Project NovelQ; contract grant number: FP6-CT-2006-015710EU.

Several protein sources have been proposed for the preparation of new thermoplastics.[1] Protein-based films, for example, can act as barriers to oxygen, carbon dioxide, oil, and fats, while mechanical and water vapor barriers properties of films produced from these materials are inferior to those of synthetic origin.[2] One of the film-forming proteins which has been object of research activity as well as of industrial interest is zein, the prolamine of corn, mainly for its unique hydrophobicity, which is due to its high content of nonpolar amino acids.[3,4] Zein is a substantially better moisture barrier than other proteins such as casein, or polysaccharides such as starch.[5] Thermoplastic processing of zein is possible if a suitable plasticizer is used in combination with heat and shear. In this way, denaturation of the hierarchical structure of zein and the development of molecular entanglements can be promoted.

The application of extrusion technologies for the production of zein films has been a challenge to researchers and few papers have been published. Wang and Padua[6] produced zein sheets plasticized with fatty acids by extruding a moldable, dough-like resin prepared by precipitating zein and oleic acid from aqueous-alcohol solutions, to finally prepare films by extrusion through a blowing head. Oliviero et al.[7] studied the feasibility of preparing thermoplastic

films of zein by direct film blowing, without the time consuming and expensive solubilization step. The zein powder was plasticized in the extruder, without the use of solvent and of a premixing phase.

Nanometric additives have been reported to dramatically change rheological properties of polymer melts and to improve functional properties such as barriers to gases and vapors, mechanical properties, and thermal stability.[8,9] Potentials and problems associated to the use of nanoscaled fillers in biopolymers for food packaging applications has been recently reviewed.[10,11] The research and development of bionanocomposite (BNC) materials for packaging applications is expected to grow in the next years, due to the possibility of improving both packaging performances and process technologies. Up to now, only few research works has dealt with the preparation of BNC made from layered silicates and proteins, including soy protein isolate,[12,13] wheat gluten,[14,15] whey protein,[12] and gelatin.[16,17]

To the best of our knowledge, there is no study in the literature on the preparation and characterization of BNC based on thermoplastic zein (TPZ) and layered silicates. The only published work on zein BNC films with clay is based on the use of solvent casting and blown extrusion technique of a resin obtained by the precipitation of zein proteins from an aqueous ethanol solutions. In the present work, the combined effect of montmorillonite (MMT) and plasticizer on the thermoplastic processing and on the properties of TPZ/MMT BNC was investigated. The structures and properties of these BNC were investigated by X-ray diffraction methods, transmission electron microscopy, thermal, dynamic-mechanical, and mechanical analyses.

EXPERIMENTAL PART

Thermoplasticization of TPZ/MMT BNC

Maize zein protein was supplied in powder form by Sigma-Aldrich (Italy). Poly(ethylene glycol) 400 (PEG) was used as plasticizer and was purchased from Fluka (Italy). The clay used in this study is unmodified sodium MMT (Cloisite Na+, supplied by Southern Clay Products, Gonzales, TX).

TPZ was processed by an internal mixer, using the following procedure. The zein powder, as received by the supplier (water content of 7 wt %) was mixed with 25 wt % PEG in a beaker using a spatula to provide a crude blend. The blend was then subjected to shear stresses in a twin counter-rotating internal mixer (Rheomix 600, Haake, Germany) connected to a control unit (Rheocord 9000, Haake, Germany), to perform the thermoplasticization. Mixing temperature, speed of rotation, and mixing time were 70°C, 50 min^{-1}, and 10 min, respectively.

TPZ/MMT BNCs were prepared in two steps. MMT was first added to the plasticizer and was stirred for 30 min to allow the intercalation of the clay platelets. The nanocomposites were then prepared by adding zein powder to the PEG/MMT systems and by using the thermoplasticization procedure described above. The amount of PEG was 25 wt % of the zein/PEG system, while the amount of clay was 1, 2.5, 5, and 10 wt % of the total composition. In the following, TPZ/MMT BNC will be indicated with the amount of MMT contained (1, 2.5, 5, 10).

After mixing, slabs to be used for further testing were produced by compression molding by using a mod LP20-B hot press (Lab Tech Engineering, Thailand). Materials were heated to and kept at 125°C at 0 bar for 7 min and at 20 bar for other 6 min and subsequently cooled in 6 min to 30°C under pressure.

TPZ and TPZ/MMT systems were subjected to X-ray diffraction (both small angle and wide angle), thermogravimetric analysis (TGA), dynamic-mechanical analysis (DMA), and tensile mechanical analysis. All of the materials were conditioned before testing at room temperature and 50% relative humidity (RH) for 2 days.

X-ray diffraction

Wide-angle X-ray diffraction (WAXS) was used to evaluate the effect of clay loading on the crystallinity of the zein phase in the TPZ and TPZ/MMT. This was performed by using a PW1710 diffractometer (Philips, Netherlands) with Cu-Kα radiation (λ = 1.54 Å) at a voltage of 40 kV and 20 mA, with a divergence slit of 1°. Samples were scanned in the range of diffraction angle 2θ = 5–40.

Small-angle X-ray scattering (SAXS) were used to characterize the morphology of BNC, by using the same diffractometer described above and setting, in this case, a divergence slit of 1/4° and the range of diffraction angle was set equal to 2θ = 2–15.

Transmission electron microscopy

Bright field transmission electron microscopy (TEM) analysis was performed on a FEI TECNAI G12 Spirit-Twin (LaB6 source) equipped with a FEI Eagle-4k CCD camera, operating with an acceleration voltage of 120 kV. Before the analysis, sections of the samples were prepared at room temperature on a Leica EM UC6/FC6 ultramicrotome and placed on 200 mesh copper grids.

Thermal analysis

TGA experiments were carried out with a TGA 2959 (TA Instruments, USA) over a temperature range from 30°C to 600°C at 10°C/min under inert atmosphere.

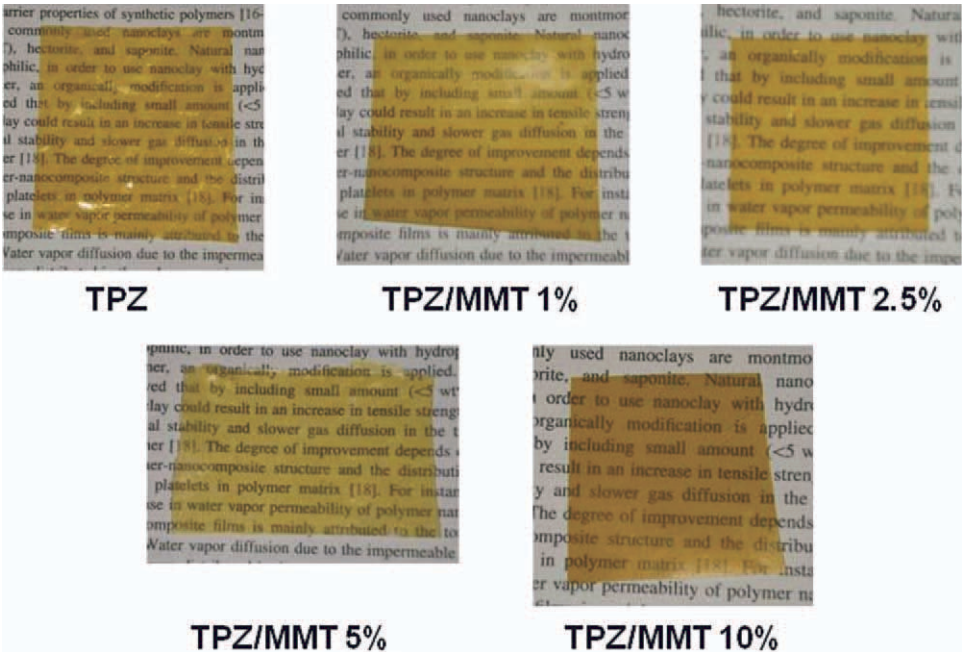

Figure 1 Photographic pictures of TPZ and TPZ/MMT BNC. [Color figure can be viewed in the online issue, which is available at wileyonlinelibrary.com.]

Dynamic-mechanical measurements

The DMA properties of the different slabs were evaluated with a dynamic mechanical analyzer Tritec 2000 (Triton Technology, Ltd., Keyworth, Notts, UK). In the single cantilever bending mode, an oscillation frequency of 1 Hz (displacement of 0.03 mm) was applied to the centre of the sample (5 mm free length) and the temperature was scanned from −70°C to 160°C at a heating rate of 2°C/min. The glass temperature transition (T_g) was determined from the maximum of the tan δ. Three runs were performed for each composition.

Tensile testing

The static tensile properties (Young modulus, stress and strain at break) were measured at room temperature with a 1 kN load cell on an Instron model 4204 (UK) tensile test machine, according to the ASTM D1708-02 on five samples for each composition.

RESULTS AND DISCUSSION

TPZ/MMT BNC

Figure 1 shows a photograph of the films obtained by compression molding. Films are glossy, yellowish, and translucent, the addition of MMT not affecting the translucency of the BNC films. Similar results were also observed by Luecha et al.[18] on zein/clay films obtained by solvent casting and extrusion blown techniques on a resin obtained by the precipitation of zein proteins from an aqueous ethanol solutions. These results suggested the good dispersion and the homogeneous distribution of the inorganic phase within the TPZ.

SAXS of TPZ, MMT, and TPZ/MMT BNC are reported Figure 2. As it can be observed, the peak characteristic of MMT layers spacing is shifted toward lower degrees in TPZ/MMT BNC containing 5 and 10 wt % of MMT with respect to TPZ, suggesting the presence of intercalated structures in the former systems (see Table I for the *d*-values of the spacings). At lower MMT concentration, this peak cannot be observed at all, indicating, possibly, a

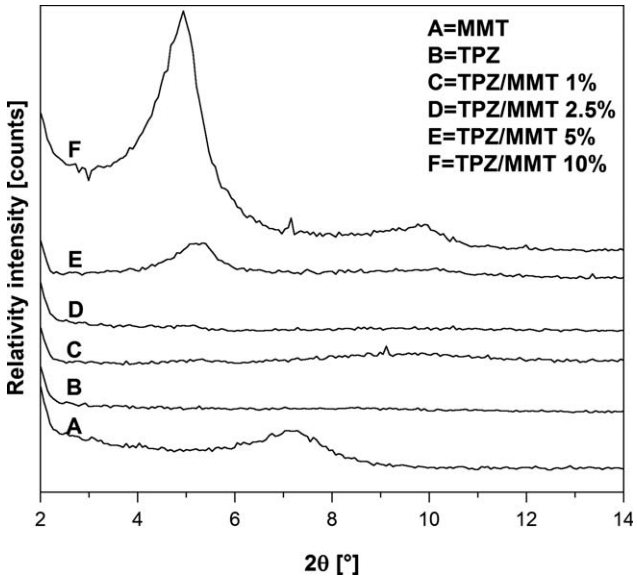

Figure 2 SAXS of TPZ, MMT, and TPZ/MMT BNC.

TABLE I
X-Ray *d*-Spacings and Peak Area Ratio for TPZ/MMT BNC

	SAXS	WAXS		
	d	A_2	A_1	A_2/A_1
MMT	12.34	–	–	–
ZEIN powder	–	10,316	17,686	0.583
TPZ	–	7106	12,048	0.590
TPZ/MMT 1%	–	2878	11,010	0.261
TPZ/MMT 2.5%	–	3345	12,200	0.274
TPZ/MMT 5%	16.45	–	11,546	–
TPZ/MMT 10%	17.57	–	15,563	–

rather extensive destructuration of the layered MMT structure occurring in these BNC. To corroborate these findings, we performed TEM measurements on TPZ/MMT BNC containing 1 wt % of clay. Figure 3 reports selected micrographs, showing both a partial intercalation of the MMT by the TPZ, which is in agreement with the increase of the *d*-spacing reported in Table I, and a good distribution of the clay within the sample.

Figure 4 shows WAXS patterns of TPZ/MMT BNC. Two characteristic peaks at $2\theta = 9.5^\circ$ and 20° can be observed, corresponding to the *d*-spacing of 9.5 (d_2) and 4.5 Å (d_1) attributed to interhelix packing and zein α-helix backbone, respectively, according to Arndt and Riley.[19]

As reported in Oliviero et al.,[7] the relative intensity of the peak at $2\theta = 9.5^\circ$ with respect to the peak at $2\theta = 20^\circ$ decreased after the thermoplasticization of the "as received" zein powder. The parameter used to evaluate the relative intensity of the two peaks was the area ratio of the peaks at $2\theta = 9.5^\circ$ and 20° (A_2/A_1). The decrease of the area ratio with thermoplasticization suggested that, while the zein helical structure resists during the thermoplasticization process, the zein molecular aggregates were disrupted. Similar conclusions were reported by Wang et al.,[20] which studied the effect of different film-forming methods on structure of zein/oleic acid films. Table I reports the area ratio (A_2/A_1) for TPZ and TPZ/MMT. In the case of TPZ/MMT BNC, the decrease of A_2/A_1 ratio with respect to the neat TPZ suggests that, during the mixing process, although zein helical structure (α-helix) resisted during the thermoplasticization process, the molecular aggregates (interhelix packing) were disrupted and the protein destructuration was more intense in the presence of MMT. This result suggests a combined effect of MMT and plasticizer on their interactions with the protein macromolecules during the mixing process, which modified the final hierarchical structure of the protein. As also observed in other natural polymer-based nanocomposite, the contemporary presence of plasticizer and clays allows for increased interactions between the nanofiller and the matrix, thus facilitating the stress transfer to the reinforcement phase, resulting in materials with improved mechanical properties.[21]

TGA are usually extensively utilized to study the thermal stability of polymeric materials. Generally, the incorporation of clay into the polymer matrix was found to enhance thermal stability by acting as a superior insulator and mass transport barrier to the volatile products generated during decomposition. Figure 5 reports a typical TGA thermogram of weight loss as function of temperature of the TPZ/MMT BNC along with neat TPZ. TGA curves showed a small weight loss in the range 30–170°C, associated to the evaporation of water, whereas a significant weight decrease started at 270°C and can be associated to the degradation of the zein/plasticizer systems. The thermal decomposition of BNC materials shifted slightly toward higher temperatures with respect to TPZ, which confirmed the enhanced thermal stability of the confined macromolecules. After 600°C, all the

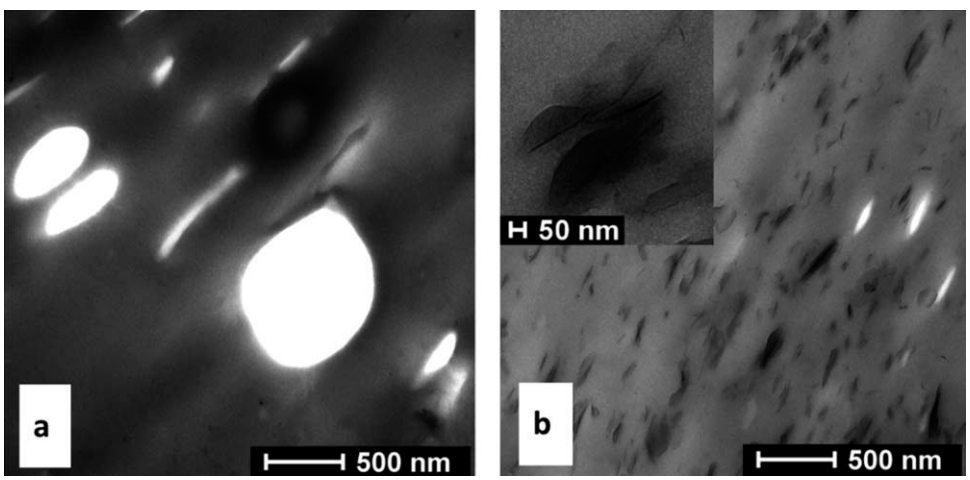

Figure 3 TEM images of: (a) neat TPZ; (b) TPZ/MMT BNC with 1 wt % MMT.

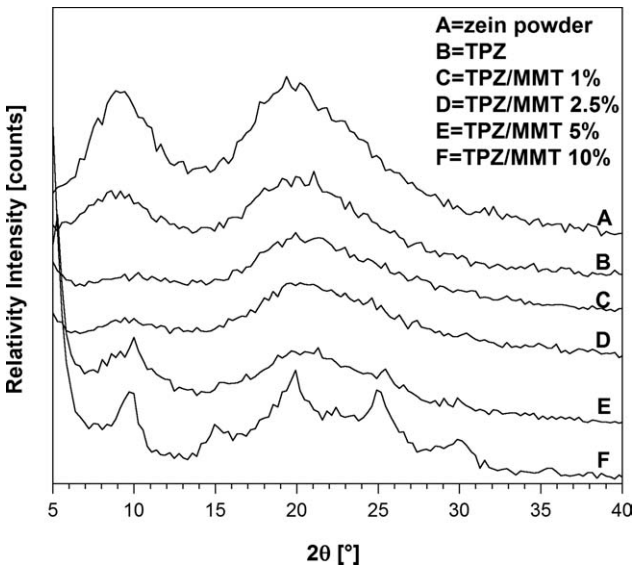

Figure 4 WAXS of TPZ/MMT BNC.

curves became flat and mainly inorganic residue remained.

Glass transition temperature, T_g

The plasticizing effect of small polar molecules such as glycerol and water in proteic systems has been widely analyzed in the literature.[22–24] The depression of T_g by the addition of a diluent or plasticizer may be explained by a number of theoretical approaches such as free volume theories or classical thermodynamic theories based on considerations of the entropies of the components at the T_g of the mixtures. In general, the T_g of a biopolymer–water–plasticizer system depends upon the T_g of the single components and their amount in the mixture.[22]

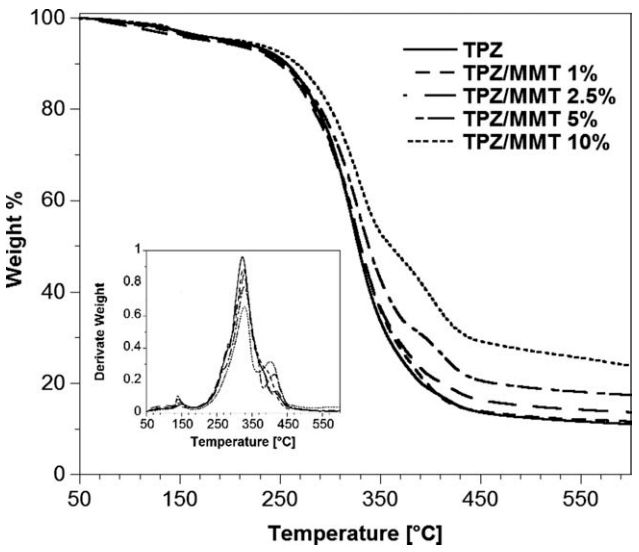

Figure 5 Thermogravimetric curves of TPZ and TPZ/MMT BNC. Inset: derivative TGA.

In the BNC analyzed in this work, the T_g can be also affected by the presence of the MMT platelets. These polar inorganic nanoparticles can interact with both the low-molecular weight plasticizers and with hydrophilic groups present in the protein macromolecules resulting in materials with different molecular mobility and thermal properties. Layered silicates offer high surface area which may represent a huge interface with the polymer matrix and may concur to bulk material properties. In a recent review on nanocomposites based on biodegradable polyesters it is shown that interactions of layered silicates with polyester chains lead to a great enhancement of thermal, mechanical, and rheological properties.[9] Negligible effects are often observed on T_g and melting temperature even though the crystallinity and crystallization kinetics can be greatly affected due to a balance between the restriction of the chain mobility and to the nucleating effects of the nanoparticles. For example, Di et al.[25] reached exfoliated state in the case of poly(ε-caprolactone) (PCL)/organoclay systems prepared by direct melt intercalation with 2–5 wt % of organoclay. They reported great enhancements of mechanical and thermal properties as well as a pseudo solid-like rheological behaviour caused by the strong interactions between the organoclay layers and PCL and by the good dispersion of exfoliated organoclay platelets. Moreover, the isothermal crystallization behaviour revealed that the well-dispersed organoclay platelets acted as nucleating agents, but also affected the crystals quality by reducing chain mobility.[25–27]

Figures 6 and 7 report representative curves for DMA measurements, showing the effect of clay concentration on the tan δ and storage modulus (E') as

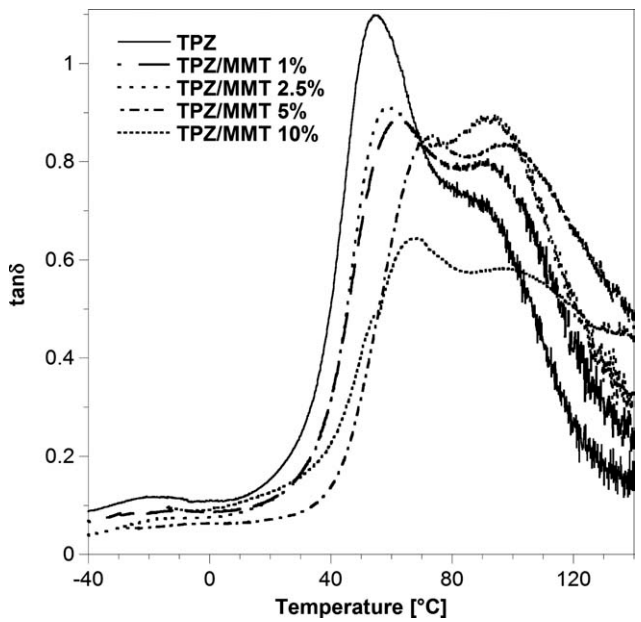

Figure 6 Tan δ of TPZ and TPZ/MMT BNC.

function of temperature for the systems under consideration. The presence of MMT modified the interactions between plasticizers and protein macromolecules with strong consequences on the viscoelastic behavior of these systems. As shown in Figure 6, the presence of MMT not only reduces the maximum values at the peaks but it induced a shift of these peaks at higher temperatures. The combined effect of MMT platelets and plasticizer affected the chain mobility of the macromolecules, resulting in plastic materials with increased T_g of the BCN with respect to neat TPZ. However, we did not observe a monotonic increase of T_g with clay content. This is due to the different scenario in terms of protein–plasticizer–clay interactions, as discussed below.

Similar effects can be also observed by analyzing the sharp drop with temperature (α-relaxation) of the storage modulus (E') exhibited at the T_g (Fig. 7). The loss observed in modulus for TPZ and TPZ/MMT BNC was about three orders of magnitude. This loss is typically observed in synthetic polymers and reflects motions of fierily long chain segments in the amorphous domains of the polymers.

It is interesting to observe that the storage modulus of BNC films can be greatly improved, even at low amount of MMT. As shown in Figure 7, an increase of storage modulus before and after the glass transition temperature was obtained by increasing the content of MMT from 1% to 5%, confirming a very good degree of exfoliation of MMT platelets in these systems.

Similar results were found, very recently, on chitosan/glycerol/clay systems.[21] The authors observed that in absence of glycerol as plasticizer, they obtained not intercalated or poorly intercalated clay stacks. In this case, they did not see any change in the thermomechanical behavior of materials in terms of both T_g and height of the tan δ peak. When glycerol was used as plasticizer, the storage modulus increased with the MMT contents in the glassy region. They suggested that the interactions between chitosan matrix and MMT platelets were strong enough to allow for an efficient load transfer between the matrix and the fillers. The T_g of the nanocomposites was slightly higher than that of neat chitosan and the area under the tan δ curves was reduced. The authors explained this result in terms of a restriction to the relaxation movements of chitosan macromolecules probably due to the higher extent of the chitosan intercalation. However, we must note that the main differences between our systems and those based on solvent casting is that during the preparation of cast films, as the case of the chitosan/glycerol/clays systems,[21] interactions between macromolecules, plasticizers, and clays develop during the evaporation of the solvent, while in our TPZ/MMT BNC these type of interactions are promoted by applying heat and shear in absence of solvents.

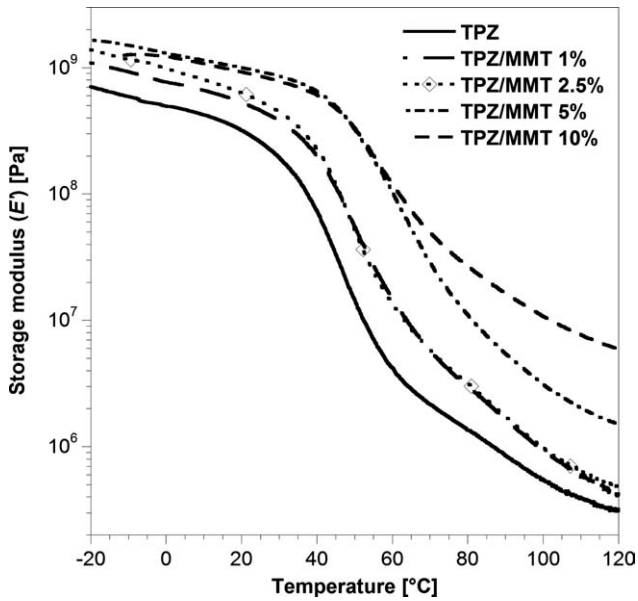

Figure 7 Storage modulus of TPZ and TPZ/MMT BNC.

We propose here the possible mechanisms that could occur in the TPZ systems that are responsible for the reduced molecular mobility of the plasticized zein. Figure 8 shows how the modification of the intra- and intermolecular interactions, caused by the combined effect of MMT and plasticizer, affect the hierarchical structure of the protein. In Figure 8(a), the presence of MMT promotes the loss of α-helix interactions, as already evidenced by the WAXS analysis. Figure 8(b) shows the possible protein–PEG–MMT interactions that lead to the possible formation of supramolecular structures that can influence the chain mobility of the disordered segments of the proteins. The Scenario A, where only protein–PEG interactions are present, schematically represent the ideal situation occurring in the absence of MMT, while Scenario B would represent the ideal situation where functional groups of proteins interacts with MMT in the absence of plasticizer molecules. Finally, Scenario C could develop when both PEG and MMT are present. It is reasonable to assume that these three situations could simultaneously be present in the zein-PEG-MMT structures. In particular, Scenario B would be responsible of the strong polymer–MMT–polymer supramolecular interactions that can behave as physical crosslinking points between different amorphous segments, thus reducing the local mobility of the protein macromolecules, resulting in materials with higher T_g and reduced tan δ. By increasing the amount of MMT in the system, the probability of Scenario B increases and, as consequence, materials with higher T_g and lower tan δ are observed.

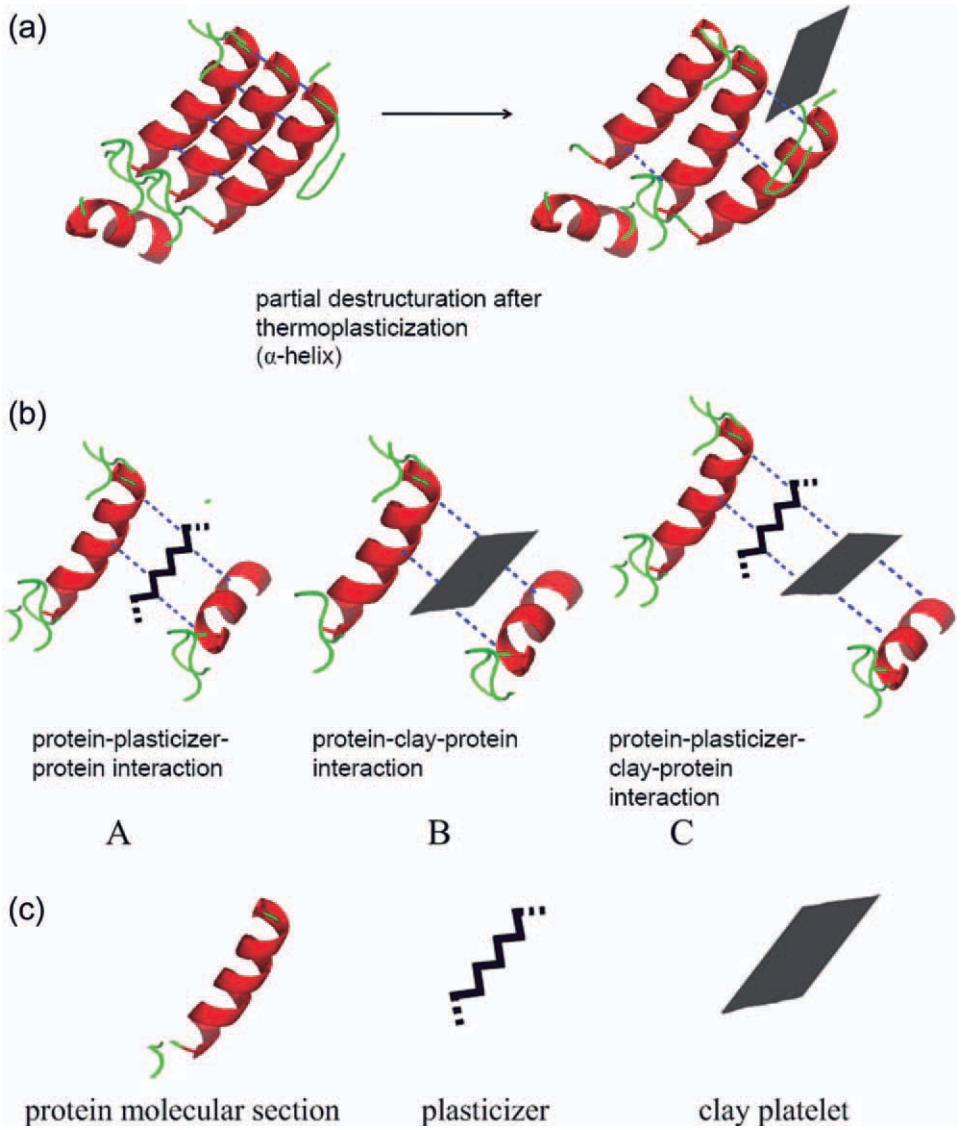

Figure 8 Schematic of the possible mechanisms involved in protein–plasticizer–MMT interaction; (a) effect of clay on the α-helix intermolecular spacing; (b) possible scenarios involving different interactions among proteins, plasticizer, and nanoplatelets; (c) species involved. [Color figure can be viewed in the online issue, which is available at wileyonlinelibrary.com.]

Moreover, in addition to the possible interactions represented by Scenarios A, B, and C, we must consider that part of the plasticizing molecules could not be made available due to the plasticizer sequestering promoted by the strong interactions with MMT nanoplatelets. The sequestering of low-molecular weight compounds by MMT would, in fact, further reduce the amount of PEG molecules involved in Scenario A, thus hindering the plasticization efficiency and promoting the increase of T_g. TEM micrographs in Figure 3 confirm this assumption. In particular, the TEM in Figure 3(a) shows the presence of PEG-rich phase in the form of small islands, which are not present, conversely, in samples containing 1 wt % MMT [Fig. 3(b)].

Mechanical properties

Mechanical properties of TPZ and TPZ/MMT BNC are summarized in Table II. As already shown for many polymer/clay nanocomposites, the tensile moduli of the TPZ/MMT BNC were remarkably improved, especially at low concentration of MMT. In most conventionally filled-polymer systems, the modulus increases linearly with the filler volume fraction, whereas for these nanoparticles much lower filler concentrations determine a sharp increase of the modulus to a much larger extent.[28,29]

It is worth to observe that, from 5 to 10 wt %, the Young's modulus of TPZ/MMT BNC increases in a less dramatic way than at lower concentration of MMT. In fact, it is well known that, beyond the

TABLE II
Tensile Properties of TPZ/MMT BNC

Material	Young modulus (MPa)	Stress max (MPa)	Stress at break (MPa)	Strain at break (mm/mm)
TPZ	296 ± 31	6.93 ± 0.57	6.68± 0.5	0.07 ± 0.0066
TPZ/MMT 1%	444 ± 25	8.93 ± 0.45	8.5 ± 0.3	0.052 ± 0.01
TPZ/MMT 2.5%	552 ± 31	9.46 ± 1.23	9.46 ± 1.23	0.042 ± 0.005
TPZ/MMT 5%	1205 ± 41	12.9 ± 0.06	12.9 ± 0.06	0.015 ± 0.002
TPZ/MMT 10%	1478 ± 351	13.98 ± 5.12	13.98 ± 5.12	0.01 ± 0.003

percolation limit, the additional silicate layers are incorporated in polymer regions that are already affected by other silicate layers, and thus it is expected that the enhancement of modulus will be reduced.

The maximum stress of the hybrids also increased remarkably with the MMT content. As discussed for the Young's modulus, the increase of the maximum stress was less dramatic above the loading of 5 wt %. The tensile data represent an important increase of 407% in the modulus and an increase in tensile strength of 186% for the 5 wt % composition. On the other hand, the elongation at break decreases almost monotonically from 7 to 1%, for MMT loading increasing from 0 (TPZ) to 10 wt % TPZ/MMT BNC.

The enhancement of the modulus for such extremely low MMT loading can be correlated to the introduction of the higher modulus inorganic filler with high aspect ratio. For examples, in the absence of plasticizers, the intercalation of 5 wt % clay in gelatine improved Young's modulus by 1.8 times as those of original gelatine.[17] These results were explained on the basis of the Halpin–Tsai (HT) equation.[30] The property enhancement was dependent on the interfacial strength between the matrix and nanofiller, the geometry or aspect ratio of the nanoparticle, and the volume fraction of the added nanoparticles.

A modified form of the HT equation (MHT) reads as follows:[31–33]

$$E/E_m = (1 + \xi\eta\phi)/(1 - \varphi\eta\phi),$$

where

$$\eta = (E_f/E_m - 1)\Big/(E_f/E_m + \xi)$$

$$\varphi = 1 + \phi\left[(1 - \phi_m)/\phi_m^2\right]$$

in which E, E_m, and E_f are the Young's moduli of the composite, the matrix, and the filler, ξ is a shape parameter dependent upon filler geometry, orientation, and loading direction and ϕ is the volume fraction of filler. φ depends on the maximum volumetric packing fraction, ϕ_m (true volume of the filler/apparent volume occupied by the filler); the original form of the HT equation is recovered if $\phi_m = 1$ and, consequently, $\varphi = 1$. In general, a better dispersion of the filler originates a larger apparent volume and a lower value of ϕ_m that results in a faster increase of the modulus ratio upon the volumetric fraction of the filler. The HT and the MHT equations, which were developed to estimate reinforcement effects of filler in composites, have been also used to predict the effect of nanoclay in nanocomposites.[32] In this case the role of ϕ_m in predicting the reinforcing effects of filler becomes important even at low filler loading, due to the very high aspect ratio of these nanoparticles. For example, Wu et al.[33] have shown that, in order to predict the Young's modulus of rubber-clay nanocomposites at volumetric fraction higher than 3% (around 10% by weight), ϕ_m needs to be in the range of 0.15–0.2. However, the HT equation was able to predict the modulus at clay concentration up to 10 wt %.

In Figure 9(a), the experimental data are compared with theoretical predictions based on both HT and MHT equations. The volumetric fraction of clay was calculated by assuming that the density of the clay is 2.6 g/cm^3 and the density of all the polymeric matrices is equal to 1.15 g/cm^3 for all the materials reported in Figure 9. This was chosen as an average value by considering that the densities of plasticizers are 1.126 g/cm^3 for PEG and 1.262 g/cm^3 for glycerol and the measured density of neat TPZ is equal to 1.102 g/cm^3. The Young's modulus of the MMT was 175 GPa.

When the HT equation is used (ϕ_m =1), experimental data up to 5 wt % of MMT can be predicted with a shape parameter ζ equal to 180. A lower value of $\zeta = 100$ must be conversely used to predict the data for 10 wt % MMT. These results indicate that, above 5%, MMT is dispersed in a less efficient way and the apparent final aspect ratio of the particles is lower. It is interesting to observe that, if we consider only the data up to 5 wt %, better predictions could be obtained by the MHT equation with a very low value of ϕ_m =0.033.

In order to further analyze the reinforcing effect of MMT in the presence of plasticizers, we have compared the Young's modulus of our TPZ/MMT BNC to those reported in the literature on gelatine/clay[31] and wheat gluten (WG)/glycerol/clay systems

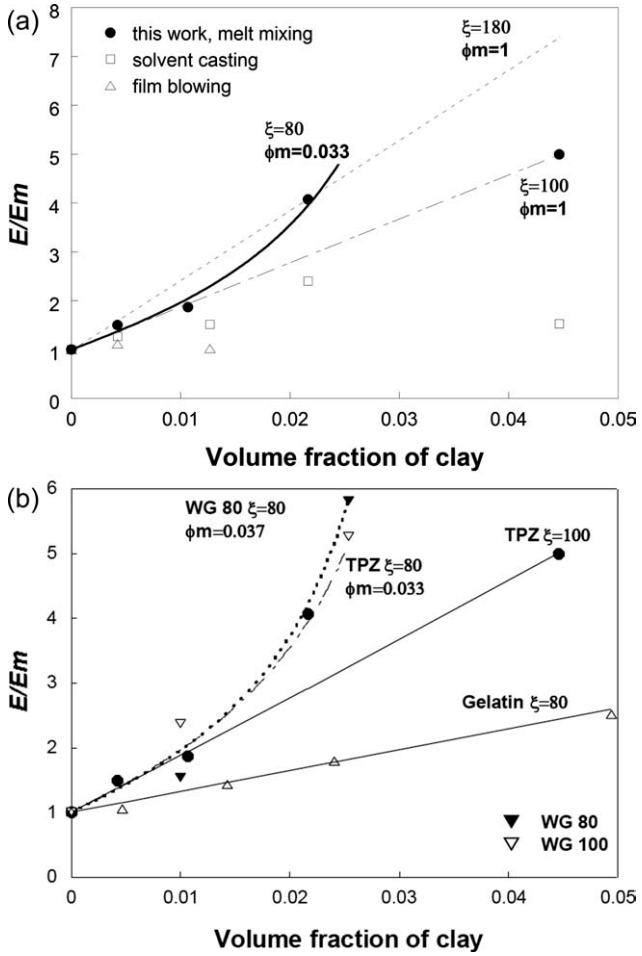

Figure 9 Relative mechanical properties of TPZ/MMT BNC and other BNC, together with results from Halpin–Tsai modelling, (a) comparison with other processing techniques; (b) comparison with other Bs data from ref. 15 and 31.

prepared at different processing conditions, in particular at 80°C (WG80) and 100°C (WG100).[15]

Data reported in Figure 9(b) show that the reinforcing efficiency in systems containing plasticizers is significantly higher compared to materials without plasticizers. In particular, experimental data of gelatine/clay systems without plasticizer can be predicted with the HT model with $\phi_m = 1$ and the aspect ratio parameter $\zeta = 80$. In plasticized materials higher aspect ratios $\zeta = 100$–200 need to be used to have a good fitting of the experimental data. It is interesting to observe that good theoretical prediction is also obtained for WG systems with the MHT equation ($\phi_m = 0.037$ and $\zeta = 80$). We should, however, consider that a packing factor of $\phi_m = 0.033$ is extremely low, when compared to the typical values found for traditional fillers in composites ($\phi_m = 0.6$–0.85) and even in rubber-clay nanocomposites ($\phi_m = 0.15$–0.2).[33] Again, this is a further evidence that we have a combined effect of reinforcing nanofillers and plasticizer through three possible mechanisms: (i) the higher degree of exfoliation that resulted in higher aspect ratio, (ii) the development of better interactions between the nanoparticles and the protein, (iii) the occurrence of possible sequestration mechanisms that could reduce the amount of plasticizers available thus leading to materials with higher rigidity.

CONCLUSIONS

BNC based on TPZ and intercalated/exfoliated MMT (1, 2.5, 5, and 10%) were successfully prepared and characterized. The protein destructuration was found to be higher in presence of the MMT nanoparticles, due to the higher shear stresses developed during the mixing process. The thermal stability of BNC films improved as content of MMT increased. The dynamic-mechanical properties showed an increase of storage modulus as well as an increase of the glass transition temperature of more than 20°C when increasing the content of MMT (without organic modification) from 1% to 5%. The tensile data showed a remarkable increase of modulus and tensile strength while the elongation at break decreases almost monotonically.

These results indicate that the presence of MMT platelets modifies the interactions between the plasticizers and the protein macromolecules. We suggest that the observed increase of T_g and the remarkable increase of the mechanical properties are due to combined effect of reinforcing nanofillers and plasticizer through three possible mechanisms: (i) the higher degree of exfoliation that resulted in higher aspect ratio, (ii) the development of better interactions between the nanoparticles and the protein macromolecules promoted by the low-molecular weight plasticizers, (iii) the occurrence of possible sequestration mechanisms that could reduce the amount of PEG available for the protein plasticization. However, further research is needed to clarify the role of these three mechanisms for the design and optimization of the properties of BNC containing low-molecular weight plasticizers.

References

1. Cuq, B.; Gontard, N.; Guilbert, S. Cereal Chem 1998, 75, 1.
2. Gennadios, A.; McHugh, T. H.; Weller, C. L.; Krochta, J. M. In Edible Films and Coatings to Improve Food Quality; Krochta, J. M., Baldwin, E. A., Nisperos-Carriedo, M.O., Eds.; Technomic Publishing Co.: Lancaster, PA, 1994; Chapter 9.
3. Reiners, R. A.; Wall, J. S.; Inglett, G. E. In Industrial Uses of Cereals; Pomeranz, Y., Ed.; Am. Assoc. Cereal Chem.: St. Paul, MN, 1973; Chapter 7.
4. Augustine, M. E.; Baianu, I. C. Food Sci 1987, 52, 649.
5. Lai, H. M.; Padua, G. W. Cereal Chem 1998, 75, 194.
6. Wang, Y.; Padua, G. W. Macromol Mater Eng 2003, 288, 886.
7. Oliviero, M.; Di Maio, E.; Iannace, S. J Appl Polym Sci 2010, 115, 277.
8. Ray, S. S.; Bousmina, M. Prog Mater Sci 2005, 50, 962.

9. Bordes, P.; Pollet, E.; Avérous, L. Prog Polym Sci 2009, 34, 125.
10. Sorrentino, A.; Gorrasi, G.; Vittoria, V. Trends Food Sci Technol 2007, 18, 84.
11. Arora A.; Padua, G. W. J Food Sci 2010, 75, 43.
12. Huang, S.; Netravali, A. N. Biomacromolecules 2006, 7, 2783.
13. Chen, P.; Zhang, L. Biomacromolecules 2006, 7, 1700.
14. Tunc, S.; Angellier, H.; Cahyana, Y.; Chalier, P.; Gontard, N.; Gastaldi, E. J Membr Sci 2007, 289, 159.
15. Angellier-Coussy, H.; Torres-Giner, S.; Morel, M. H.; Gontard, N.; Gastaldi, E. J Appl Polym Sci 2008, 107, 487.
16. Martucci, J. F.; Vazquez, A.; Ruseckaite, R. A. J Therm Anal Calorim 2007, 89, 117.
17. Zheng, J. P.; Li, P.; Ma, L. Y.; Yao, K. D. J Appl Polym Sci 2002, 86, 1189.
18. Luecha, J.; Sozer, N.; Kokini, J. L. J Mater Sci 2010, 45, 3529.
19. Arndt, U. W.; Riley, D. P. Philos Trans R Soc (London) A 1955, 247, 409.
20. Wang, Q.; Wang, J. F.; Geil, P. H.; Padua, G. W. Biomacromolecules 2004, 5, 1356.
21. Lavorgna, M.; Piscitelli, F.; Mangiacapra, P.; Buonocore, G. Carbohydr Polym 2010, 82, 291.
22. Hernandez-Izquierdo, V. M.; Krochta, J. M. J Food Sci 2008, 73, 30.
23. Di Gioia L.; Guilbert, S. J Agric Food Chem 1999, 47, 1254.
24. Sothornvit, R.; Krochta J. M. In Innovations in Food Packaging; Han J. H., Ed.; Academic Press: UK, 2005; Chapter 23.
25. Di, Y.; Iannace, S.; Di Maio, E.; Nicolais, L. J Polym Sci Polym Phys 2003, 41, 670.
26. Di Maio, E.; Iannace, S.; Sorrentino, L.; Nicolais, L. Polymer 2004, 45, 8893.
27. Chen, G. X.; Yoon, J. S. J Polym Sci Part B: Polym Phys 2005, 43, 817.
28. Sinha Ray, S.; Okamoto, M. Prog Polym Sci 2003, 28, 1539.
29. Shia, D.; Hui, C. Y.; Burnside, S. D.; Giannelis, E. P. Polym Compos 1998, 19, 608.
30. Halpin, J. C. J Compos Mater 1969, 3, 732.
31. Rao, Y. Q. Polymer 2007, 48, 5369.
32. Fornes, T. D.; Paul, D. R. Polymer 2003, 44, 4993.
33. Wu, Y.-P.; Jia, Q.-X.; Yu, D.-S.; Zhang, L.-Q. Polym Test 2004, 23, 903.